AIAA JOURNAL
Vol. 31, No. 10, October 1993

Low-Reynolds-Number k-ε Model for Unsteady Turbulent Boundary-Layer Flows

Sixin Fan* and Budugur Lakshminarayana†
Pennsylvania State University, University Park, Pennsylvania 16802
and
Mark Barnett‡
United Technologies Research Center, East Hartford, Connecticut 06108

An assessment of the near-wall and low-Reynolds-number functions used in low-Reynolds-number k-ε models suggests that they are not suitable for the near-wall region of unsteady turbulent boundary layers, where the flow is characterized by rapid changes in phase. An improved low-Reynolds-number k-ε model is developed in this paper. The near-wall and low-Reynolds-number functions in this model are formulated as functions of the local turbulent Reynolds numbers instead of the inner variable y^+. The present model also has the correct asymptotic behavior in the near-wall region. The turbulence model has been incorporated in an unsteady boundary-layer code and validated for unsteady turbulent boundary layers with and without adverse pressure gradients. The predictions agree well with the experimental data and the theoretical analysis. For the cases tested, the present model correctly predicts the unsteady near-wall flow and the unsteady skin friction at various frequencies.

Nomenclature

C_f = friction coefficient, $\tau_w/(0.5\rho_0\bar{u}_0^2)$
f = frequency, Hz
H = total enthalpy
k = turbulence kinetic energy $0.5(\tilde{u}^2+\tilde{v}^2+\tilde{w}^2)$
l_s^+ = near-wall similarity parameter, $l_s^+ = \sqrt{(2\nu/\omega)}\,(\bar{u}_\tau/\nu)$
P_r, P_{rt} = molecular and turbulent Prandtl numbers
p = static pressure
Re = Reynolds number, $\bar{u}_0 L/\nu$, L is the length of test section
R_t, R_y = turbulent Reynolds numbers, $k^2/\nu\varepsilon$, $\sqrt{k}y/\nu$
T_{ue} = freestream turbulence intensity
t = time
u, v, w = velocity components in x, y, z directions
u_τ = friction velocity, $\sqrt{\tau w/\rho}$
u^+ = nondimensional velocity, $\tilde{u}/u_\tau$
x, y, z = streamwise (from leading edge), normal, and tangential coordinates, respectively
y_s = Stokes coordinate, $y_s = y/\sqrt{2\nu/\omega}$
y^+ = inner variable, $u_\tau y/\nu$
δ, δ^*, θ = boundary layer, displacement, and momentum thickness, respectively
ε = dissipation rate of turbulent kinetic energy
μ, μ_t = molecular and turbulent eddy viscosity, respectively
ν = kinematic viscosity
ρ = density
$\sigma_k, \sigma_\varepsilon$ = turbulent Prandtl numbers for k and ε
ω = angular frequency, $2\pi f$

Subscripts

e = freestream quantity
t = turbulence quantity
w = quantity at the wall
0 = freestream quantity at the inlet

Superscripts

$\bar{}$ = time averaged quantity
$\tilde{}$ = ensemble averaged quantity
$'$ = turbulent fluctuating quantity
Amp[ ] = amplitude of the first Fourier component
Phs[ ] = phase angle of the first Fourier component

Received March 17, 1992; revision received Dec. 9, 1992; accepted for publication Dec. 14, 1992.

*Graduate Assistant. Member AIAA.
†Evan Pugh Professor of Aerospace Engineering. Fellow AIAA.
‡Research Engineer. Member AIAA.

Introduction

THE numerical simulation of unsteady turbulent flows is being attempted by many researchers due to its importance in engineering applications. Unsteady viscous flows are of significant interest in both external flows (e.g., on helicopter rotors) and internal flows (e.g., on turbomachinery blades). The applicability of the existing turbulence models to unsteady turbulent flows has not been fully investigated. Algebraic eddy viscosity models are used in most of the unsteady viscous codes, because they are numerically robust and efficient. In unsteady turbulent flows, where unsteady transport of turbulence plays an important role, the algebraic eddy viscosity models have been found inaccurate for the prediction of unsteady flow physics, such as the pseudoperiodicity in the evolution of unsteady integral parameters in a flat plate turbulent boundary layer and the phase shift of wall shear stress.[1,2]

Several investigators have applied the k-ε model for unsteady turbulent boundary layers.[1,3,4] An instantaneous logarithmic law does not generally exist in the near-wall region of unsteady turbulent wall bounded flows.[1] Hence, simple wall functions based on the logarithmic law and the equilibrium turbulence assumption are not appropriate. Cousteix and Houdeville[1] used a steady wall function with a high-Reynolds-number k-ε model for a periodic turbulent boundary layer but failed to predict the unsteady wall shear stress. Similarly, Mankbadi and Mobark[3] used a high-Reynolds-number k-ε model and steady wall functions to predict pipe and boundary-layer flows. It has been found that the accuracy of the model deteriorates with increasing level or rate of unsteadiness. Low-Reynolds-number form turbulence models seem to be necessary for accurate prediction of unsteady turbulent wall bounded flows where the near-wall physics is of interest. The applicability of the low-Reynolds-number k-ε models to unsteady flows has been investigated by Justesen and Spalart[4] for an oscillatory turbulent boundary layer with a zero mean velocity. Two different low-Reynolds-number k-ε models are used.[5,6] Comparison with large eddy simulation data indicates that Jones and Launder's[5] model performs better than Chien's[6] model. It is also shown that the pre-

Table 1 Near-wall and low-Reynolds-number functions for k-ε

	f_μ	f_1	f_2	D	E
Jones and Launder[5]	$\exp[-2.5/(1+R_t/50)$	1.0	$1-0.3\exp(-R_t^2)$	$2\nu(\partial\sqrt{k}^2/\partial y)$	$2\nu\nu_t(\partial^2\tilde{u}/\partial y^2)^2$
Chien[6]	$1-\exp(-0.0115y^+)$	1.0	$\{1-(2/9)\exp[-(R_t/6)^2]\}$	$2\nu(k/y^2)$	$-2\nu(\varepsilon/y^2)\exp(-0.5y^+)$
Lam and Bremhorst[18]	$[1-\exp(-0.0165R_y)]^2(1+20.5/R_t)$	$1+(0.05/f_\mu)^3$	$1-\exp(-R_t^2)$	0.0	0.0
Myong and Kasagi[19]	$(1+3.45/\sqrt{R_t})\times[1-\exp(-y^+/5)]$	1.0	$\{1-(2/9)\exp[-(R_t/6)^2\}$ $\times[1-\exp(-y^+/5)]^2$	0.0	0.0
Nagano and Hishida[20]	$[1-\exp(-y^+/26.5)]^2$	1.0	$1-0.3\exp(-R_t^2)$	$2\nu(\partial\sqrt{k}^2/\partial y)^2$	$2\nu\nu_t(1-f_\mu)(\partial^2\tilde{u}/\partial y^2)^2$

diction of unsteady wall shear stress from either model is unsatisfactory, and it can be improved by using a more accurate low-Reynolds-number function.

Application of full Reynolds stress models to unsteady turbulent wall flows has also been attempted by some investigators (Hanjalic and Stosic.[7–9] The model used by Ha Minh et al.[9] has a low-Reynolds-number form. It is used to predict an oscillatory boundary layer with a zero mean velocity, and the results have been compared with those from the direct numerical simulation (DNS). Although the full Reynolds stress model can predict the anisotropy of the turbulence, the accuracy of the predicted unsteady wall shear stress is not better than that computed by Justesen and Spalart[4] for a similar flow using the k-ε models. It is believed that most of the previously mentioned full Reynolds stress models suffer from insufficient near-wall treatment. Furthermore, the increased computational time to solve the additional stress transport equations is unacceptable for most engineering applications.

The empirical functions used in the low-Reynolds-number k-ε models are developed mainly for steady wall bounded turbulent flows. The unsuccessful predictions of unsteady wall friction in unsteady wall turbulent flows based on these functions, reported by Cousteix et al.[10] (using Jones and Launder's[5] model) and Justesen and Spalart,[4] suggest that the existing near-wall and low-Reynolds-number functions may be insufficient for unsteady flows.

In this paper, based on some well-observed features in the near-wall region of unsteady wall flows, it is argued that the inner variable y^+ is not a proper variable in the formulation of near-wall and low-Reynolds-number functions. The rapid phase changes across the near-wall region may also place a requirement on the correct near-wall asymptotic behavior of turbulence quantities and the consistency of the ε equation. The near-wall and low-Reynolds-number functions used in some low-Reynolds-number k-ε models are examined on their applicability to unsteady turbulent flows. It is found that some of the functions are not suitable for unsteady near-wall turbulent flows, where substantial variation in phase shift of flow and turbulence quantities exists, especially at high frequencies. A new model with improved near-wall and low-Reynolds-number functions is developed in this paper. These functions are based on the local turbulent velocity scale instead of the wall friction velocity and have the correct near-wall asymptotic behavior of turbulence quantities.

The turbulence model is validated against data in steady and unsteady turbulent boundary layers with zero pressure gradient.[1,11–13] Good predictions of unsteady wall shear stress have been obtained. The frequency dependency of near-wall unsteady turbulent flowfield has been investigated. The near-wall solutions have been compared with the data of Binder et al.[14] for an unsteady channel flow and the analysis of Cousteix and Houdeville.[1] The near-wall unsteady flowfield and the unsteady wall shear stress are predicted well at different frequencies. Finally, the unsteady turbulent boundary layer with adverse pressure gradient, measured by Parikh et al.,[15,16] has been computed using the new model, and good agreement is shown in both the outer region and the inner region of the boundary layer.

Assessment of Near-Wall and Low-Reynolds-Number Functions

The low-Reynolds-number k-ε equations suggested by Patel et al.[17] are given by

$$\tilde{\rho}\frac{\partial k}{\partial t}+\tilde{\rho}\tilde{u}\frac{\partial k}{\partial x}+\tilde{\rho}\tilde{v}\frac{\partial k}{\partial y}=\frac{\partial}{\partial y}\left[\left(\mu+\frac{\mu_t}{\sigma_k}\right)\frac{\partial k}{\partial y}\right]+\mu_t\left(\frac{\partial\tilde{u}}{\partial y}\right)^2-\tilde{\rho}\varepsilon-\tilde{\rho}D \tag{1}$$

$$\tilde{\rho}\frac{\partial \varepsilon}{\partial t}+\tilde{\rho}\tilde{u}\frac{\partial \varepsilon}{\partial x}+\tilde{\rho}\tilde{v}\frac{\partial \varepsilon}{\partial y}=\frac{\partial}{\partial y}\left[\left(\mu+\frac{\mu_t}{\sigma_\varepsilon}\right)\frac{\partial \varepsilon}{\partial y}\right]$$
$$+C_{\varepsilon 1}f_1\frac{\varepsilon}{k}\mu_t\left(\frac{\partial\tilde{u}}{\partial y}\right)^2-\tilde{\rho}C_{\varepsilon 2}f_2\frac{\varepsilon^2}{k}+\tilde{\rho}E \tag{2}$$

where

$$\mu_t=\rho C_\mu f_\mu\frac{k^2}{\varepsilon} \tag{3}$$

k and ε are the turbulent kinetic energy and dissipation rate and μ and μ_t are molecular and turbulent eddy viscosity.

The five constants C_μ, σ_k, σ_ε, $C_{\varepsilon 1}$, and $C_{\varepsilon 2}$ are based on high-Reynolds-number k-ε models. The near-wall and low-Reynolds-number functions f_μ, f_1, f_2, D, and E proposed by several investigators[5,6,18–20] for steady turbulent flows are given in Table 1.

In an unsteady turbulent wall bounded flow, the near-wall region is characterized by a rapid phase change in flow quantities. As observed by Binder et al.[14,21] and Cousteix and Houdeville,[1] the laminar Stokes solution represents the boundary-layer flow in the near-wall region, and the outer part of the turbulent boundary layer becomes almost frozen at high frequencies (say l_s^+ of order 5). The unsteady shear stress at the wall leads the outer flow by a phase of 45 deg. As frequency decreases, the unsteady layer penetrates into and interacts with the outer turbulent flow. It is suggested by Cousteix and Houdeville[1] that the phase angle of the unsteady velocity in the viscous sublayer decreases rapidly with increasing normal distance even at relatively low frequencies.

Two major effects are caused by the rapid change in phase of the flow quantities near the wall. First, the unsteady wall shear stress is out of phase with the flow and turbulence quantities away from the wall. As suggested by Cousteix and Houdeville,[1] the friction velocity, which has been successfully used as a characteristic velocity scale in the near-wall region of steady turbulent flows, is no longer a good parameter for the near-wall region of unsteady turbulent flows, especially at high frequencies. Consequently, the inner variable y^+, which has been widely used in formulating the near-wall and low-Reynolds-number functions for steady wall turbulent flows, is no longer suitable for unsteady flows. Hanjalic and Stosic[7] suggested that the local turbulent velocity defined as $\sqrt{k}$ may be a better velocity scale for the correlation of the logarithmic law in unsteady wall bounded turbulent flows. It is believed that the local turbulence characteristic velocity $\sqrt{k}$ is a better velocity scale in the formulation of the near-wall and low-Reynolds-number functions for unsteady turbulent wall bounded flows. In other words, parameters such as the turbulent Reynolds number $R_y=\sqrt{k}y/\nu$ or $R_t=k^2/\nu\varepsilon$ instead of y^+ should be used in the near-wall and low-Reynolds-number functions in models for unsteady turbulent flow.

The second effect is a more stringent requirement on the near-wall and low-Reynolds-number functions for the asymptotic behavior of turbulence quantities as the wall is approached. In unsteady wall bounded turbulent flow, the near-wall unsteady flow phenomena such as the phase shift in the wall shear stress is important in engineering applications. Since at high frequencies the thickness of the unsteady layer can be of the same order of the viscous sublayer, incorrect near-wall asymptotic behavior of a turbulence model may result in inaccurate prediction of near-wall unsteady turbulent stresses. In the vicinity of the wall, the analysis on the near-wall asymptotic behavior of turbulence quantities for steady wall turbulent flow gives $u'=O(y)$, $v'=O(y^2)$, $w'=O(y)$, $k=O(y^2)$, $\varepsilon=O(1)$, $\overline{u'v'}=O(y^3)$, and $\nu_t=O(y^3)$ (Ref. 17). Addi-

tional research is needed to resolve the near-wall behavior of time-dependent turbulence quantities in unsteady wall flow.

In summary, in modeling for unsteady wall bounded turbulent flow, the near-wall and low-Reynolds-number functions of a k-ε model should be formulated as functions of turbulent Reynolds numbers such as R_y or R_t, instead of y^+. These functions should ensure the correct near-wall asymptotic behavior of turbulence quantities.

The model by Jones and Launder[5] is the first proposal of low-Reynolds-number k-ε model for near-wall and low-Reynolds-number turbulent flow. This model has been widely used for steady turbulent flow in the past. The model has been found to predict a lower peak of k in flat plat boundary layer.[6,18] This result might be due to the form of the term E used in the ε equation.[17] Many improvements have been made on the near-wall and low-Reynolds-number functions since the original proposal of Jones and Launder,[5] which resulted in more accurate predictions.[6,18–20] Although Jones and Launder's[5] model does not use y^+ in its low-Reynolds-number functions, the success of this model for unsteady flow is expected to be limited by the relatively inaccurate near-wall and low-Reynolds-number functions, such as f_μ. This limitation is partly confirmed by the work of Cousteix et al.[10] and Justesen and Spalart.[4]

As shown by Patel et al.,[17] Chien's[6] model is asymptotically consistent in the near-wall region. The functions f_μ and E are correlated to y^+. This correlation is not suitable for unsteady near-wall turbulent flow, as discussed earlier. The function f_2, which models the low-Reynolds-number effects on the destruction term in the ε equation, is based on the final period of decay of isotropic turbulence. It is a function of turbulent Reynolds number and will likely remain the same form for unsteady flow.

The major deficiency of Lam and Bremhorst's[18] model lies in its asymptotic inconsistency in the near-wall region. It is shown by Patel et al.[17] that the function f_μ used in this model is of $O(1)$. This results in a turbulent shear stress of $O(y^4)$ instead of $O(y^3)$. The near-wall asymptotic consistency of the ε equation requires the function f_2 to be of $O(y^2)$. However, in this model f_2 is of $O(y^8)$. Furthermore, it is pointed out by Patel et al.[17] that the function f_2 in this model excludes the prediction of the final stage of isotropic turbulence. Although the effect of near-wall inconsistency of the model on the prediction of global flow properties is still unclear, it may result in numerical difficulties. Lai and So[22] reported difficulty in obtaining a convergent solution using Lam and Bremhorst's[18] model. They traced the difficulty to an imbalance in the ε equation in the near-wall region. Similar convergence difficulty is experienced in the present investigation. It is believed that improved treatment of the near-wall ε equation such as those proposed by Myong and Kasagi[19] are necessary for both steady and unsteady flows.

Improvements on the near-wall asymptotic behavior have been achieved by Myong and Kasagi.[19] However, the use of the variable y^+ in the functions f_μ and f_2 makes it unsuitable for unsteady wall turbulent flow. Similarly, the function f_μ in Nagano and Hishida's[20] model is also based on y^+. An analysis similar to that used by Patel et al.[17] indicates that this model will result in a near-wall shear stress of $O(y^5)$, which is incorrect.

It should be pointed out that Chien's[6] model, Myong and Kasagi's[19] model, and Nagano and Hishida's[20] model are not valid when the wall shear stress reduces to zero. This happens at a separation point or at certain phase angles in regions of an unsteady boundary layer where flow reversal exists during part of the period. When wall shear stress is zero, the inner variable y^+ as well as the friction velocity becomes zero for any value of y. These models give a zero f_μ and hence a zero eddy viscosity even for the outer region of the flow, which is incorrect. The same problem is anticipated in other y^+ based models, such as the algebraic eddy viscosity models using the Van Driest damping.

The preceding assessment indicates that the low-Reynolds-number k-ε models developed for steady flow either use the inner parameter y^+ in the near-wall and low-Reynolds-number functions or have incorrect or inaccurate near-wall behavior. A model based on the local turbulence quantities instead of y^+ and having correct near-wall behavior is therefore necessary for unsteady wall-bounded turbulent flows.

Development of a New Model

In the vicinity of the wall, the presence of the solid wall causes preferential damping of the normal component of turbulent velocity. At the same time, the turbulence motion is restricted and the Reynolds number becomes small. In the development of the near-wall and low-Reynolds-number functions, the wall damping effects and the low-Reynolds-number effects are treated separately.

In Myong and Kasagi's[19] model, a function of the form $[1-\exp(-y^+/C)]$ has been used to account for the near-wall damping effects. In a similar, but more general, way we define a new function f_w given by

$$f_w = 1 - \exp\left\{-\frac{\sqrt{R_y}}{2.30} + \left(\frac{\sqrt{R_y}}{2.30} - \frac{R_y}{8.89}\right)\left[1 - \exp\left(-\frac{R_y}{20}\right)\right]^3\right\} \quad (4)$$

For steady flow f_w is a numerical reformulation of $[1-\exp(-y^+/4.9)]$, which is suggested by Speziale et al.[23] The data by Patel et al.[17] are used in formulating Eq. (4) in terms of R_y. The use of R_y instead of y^+ in the preceding expression makes it suitable for unsteady flow. The function f_w is of $O(y)$ in the vicinity of the wall. In the present model f_w is used as a near-wall function to account for the wall damping effects. For example, f_w^2 is used when a second-order damping is required.

According to Myong and Kasagi's[19] dimensional analysis, the characteristic turbulence length scale is $\sqrt{\nu k/\varepsilon}$ in the proximity of the wall, due to the effects of small turbulent Reynolds number. Thus the eddy viscosity reduces to $k\sqrt{\nu/\varepsilon}$, or $k^2/\varepsilon\sqrt{R_t}$. At high Reynolds number and far from the wall, the eddy viscosity scales as k^2/ε. The preferential wall damping effects have not been taken into account in the above analysis. To achieve the correct near-wall asymptotic behavior of turbulent eddy viscosity, that is, $\nu_t = O(y^3)$, the function f_w should be multiplied to give an eddy viscosity of $\nu_\tau \sim f_w k^2/\varepsilon\sqrt{R_t}$ in the near-wall and low-Reynolds-number limit. A function f_μ is needed to interface the near-wall low-Reynolds-number eddy viscosity and the high-Reynolds-number eddy viscosity. The function f_μ should approach $f_w/\sqrt{R_t}$ at the near-wall and low-Reynolds-number limit and unity at the high-Reynolds-number limit. Using the data of Patel et al.[17] for steady wall turbulent flows, the following empirical correlation for f_μ has been derived:

$$f_\mu = 0.4\frac{f_w}{\sqrt{R_t}} + \left(1 - 0.4\frac{f_w}{\sqrt{R_t}}\right)\left[1 - \exp\left(-\frac{R_y}{42.63}\right)\right]^3 \quad (5)$$

The three constants in the preceding expression have been optimized to give good agreement with the data by Patel et al.[17] Figure 1 shows the comparison of the present formula with those of Lam and Bremhorst's[18] model and Myong and Kasagi's[19] model. The function in Jones and Launder's[5] model and Chien's[6] model are

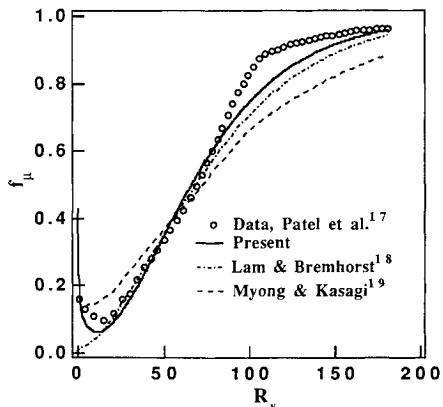

Fig. 1 Comparison of the function f_μ from different models.

not compared in Fig. 1 because a different asymptotic behavior is required for f_μ in their models due to the different definition for the dissipation rate. It can be seen that the present expression accurately represents the trend of the data, especially at the near-wall and low-Reynolds-number limit.

The function f_1 has been assumed as unity in the present model, as suggested by Myong and Kasagi[19] and Speziale et al.[23] The function f_2 is used to account for the low-Reynolds-number effects on the destruction term in the dissipation equation. The formula due to Hanjalic and Launder,[24] multiplied by a near-wall damping function of f_w^2, is used in the present model,

$$f_2 = \left\{1.0 - \frac{0.4}{1.8}\exp\left[-\left(\frac{R_t}{6}\right)^2\right]\right\} f_w^2 \tag{6}$$

The damping factor f_w^2 is used to ensure the near-wall balance of the dissipation equation. The correction functions D and E are chosen as zero. Accordingly, the boundary conditions are $k = 0$, $\partial\varepsilon/\partial y = 0$ at $y = 0$.

The value of the five model constants are as follows: $C_\mu = 0.09$, $\sigma_k = 1.0$, $\sigma_\varepsilon = 1.3$, $C_{\varepsilon 2} = 1.8$. $C_{\varepsilon 1}$ is calculated from the relation given by Patel et al.,[17]

$$C_{\varepsilon 1} = C_{\varepsilon 2} - (\kappa^2/\sigma_\varepsilon C_\mu^{1/2}) \tag{7}$$

with $\kappa = 0.4$, $C_{\varepsilon 1}$ is approximately 1.4.

In the present model, the near-wall and low-Reynolds-number functions are related to local turbulent Reynolds numbers instead of the inner variable y^+ and the near-wall asymptotic behaviors are ensured.

Numerical Solution Procedure

The unsteady compressible boundary-layer procedure and the code developed by Power et al.[2] are used. The governing equations are the continuity equation, the streamwise momentum equation, and the total enthalpy equation,

$$\frac{\partial\tilde{\rho}}{\partial t} + \frac{\partial(\tilde{\rho}\tilde{u})}{\partial x} + \frac{\partial(\tilde{\rho}\tilde{v})}{\partial y} = 0 \tag{8}$$

$$\tilde{\rho}\frac{\partial\tilde{u}}{\partial t} + \tilde{\rho}\tilde{u}\frac{\partial\tilde{u}}{\partial x} + \tilde{\rho}\tilde{v}\frac{\partial\tilde{u}}{\partial y} = -\frac{\partial\tilde{p}}{\partial x} + \frac{\partial}{\partial y}\left[(\mu + \mu_t)\frac{\partial\tilde{u}}{\partial y}\right] \tag{9}$$

$$\tilde{\rho}\frac{\partial\tilde{H}}{\partial t} + \tilde{\rho}\tilde{u}\frac{\partial\tilde{H}}{\partial x} + \tilde{\rho}\tilde{v}\frac{\partial\tilde{H}}{\partial y} = \frac{\partial\tilde{p}}{\partial t} + \frac{\partial}{\partial y}$$

$$\times\left[\mu\left(1 - \frac{1}{P_r}\right)\tilde{u}\frac{\partial\tilde{u}}{\partial y} + \left(\frac{\mu}{P_r} + \frac{\mu_t}{P_{rt}}\right)\frac{\partial\tilde{H}}{\partial y}\right] \tag{10}$$

A constant value of 0.95 is used for P_{rt} in the following computations. The boundary-layer equations are transformed using a modified Levy-Lees transformation. A fully implicit numerical scheme has been used to solve the transformed equations (see Power et al.[2] for detailed description). A similar numerical procedure has been used in the present study to solve the k-ε equations.

The computation starts from a laminar solution. The empirical k, ε profiles suggested by Schmidt and Patankar[25] are prescribed at the second streamwise station

$$k = k_e(\tilde{u}/\tilde{u}_e)^2 \tag{11}$$

$$\varepsilon = 0.1k(\partial\tilde{u}/\partial y) \tag{12}$$

$$k_e = 1.5(T_{ue}\tilde{u}_e)^2 \tag{13}$$

where T_{ue} is the freestream turbulence intensity, and k_e is the freestream turbulence kinetic energy. The boundary layer becomes fully turbulent after a short transition region.

Results and Discussion

Steady Turbulent Boundary Layer

To validate the present turbulence model, which should work well for both steady and unsteady turbulent flows, the steady turbulent boundary measured by Wieghardt and Tillmann[11] has been computed. This case has been widely used to test turbulence models.[17,19,23] In the streamwise direction 201 grid points are used, and in the normal direction 161 grid points are used, with the first grid lying at $y^+ < 1$.

The wall friction coefficient is compared with the experimental data in Fig. 2. The agreement is very good. At $x = 0.4987$ m, the computed C_f is 0.00241 as compared to the experimental value of 0.00243. The velocity profile and near-wall turbulence quantities are compared in Fig. 3. The predicted velocity approaches the linear profile $u^+ = y^+$ in the viscous sublayer and the logarithmic distribution of $u^+ = 1/0.418\ \ln y^+ + 5.5$ in the logarithmic region, as suggested by Patel et al.[17] The near-wall asymptotic behavior of turbulence quantities has been correctly predicted. Good agreement between the predicted k and shear stress profiles and the data of Patel et al.[17] is also achieved. The predicted ε profile has a lower peak than the data. This is believed acceptable considering the fact that recent DNS data show a different near-wall trend of ε than that of the measured data.

Unsteady Turbulent Boundary Layers on a Flat Plate

The unsteady turbulent boundary layer on a flat plate measured by Cousteix and Houdeville[1] has been computed using both the present model and Chien's[6] model. The freestream velocity is given as

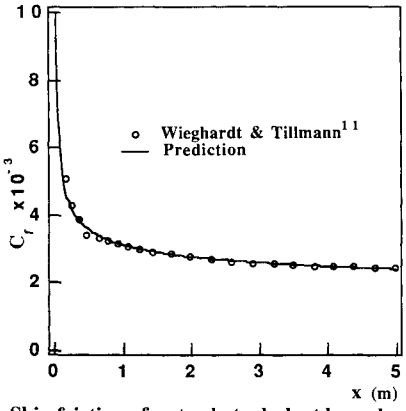

Fig. 2 Skin friction of a steady turbulent boundary layer.

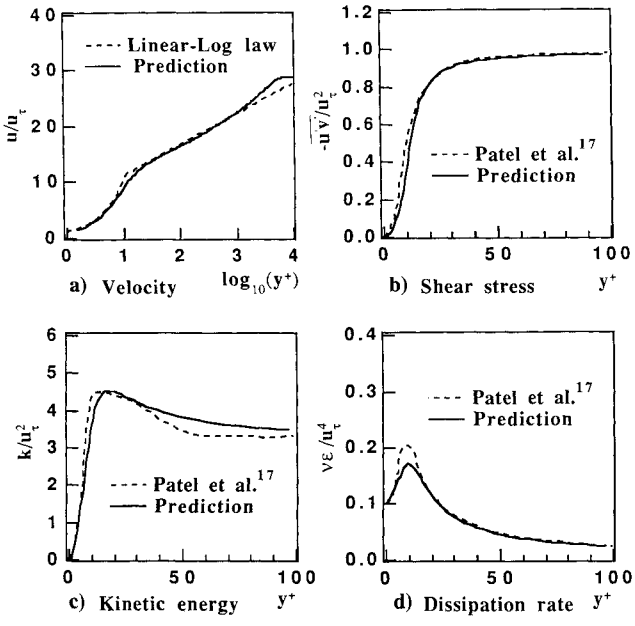

Fig. 3 Velocity and turbulence profiles in a steady boundary layer ($x = 4.987$ m).

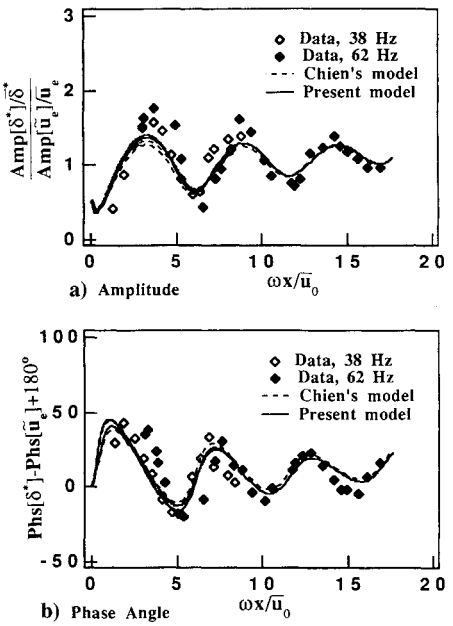

Fig. 4 Amplitude and phase angle of displacement thickness in an unsteady turbulent boundary layer (data: Cousteix and Houdeville[1]).

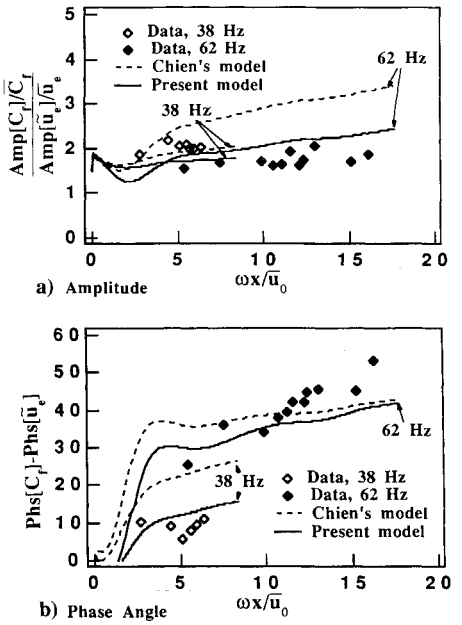

Fig. 5 Amplitude and phase angle of friction coefficient in an unsteady turbulent boundary layer (data: Cousteix and Houdeville[1]).

$$u_e = u_e[1 + A \sin(\omega t + \mathrm{Phs}[u_e])] \tag{14}$$

For the low-frequency case, $f = 38$ Hz, $\bar{u}_e = 21.9$ m/s,

$$\mathrm{Phs}[\tilde{u}_e] = 7.6(x - 0.047) \text{ (deg)} \tag{15}$$

$$A = 0.152 - 0.0743(x - 0.047) \tag{16}$$

where x is measured from the leading edge, $\omega = 2\pi f$.

For the high-frequency case, $f = 62$ Hz, $[\tilde{u}_e] = 16.8$ m/s,

$$\mathrm{Phs}[\tilde{u}_e] = [88.9(x - 0.047)^2 + 6.66(x - 0.047)] \text{ (deg)} \tag{17}$$

$$A = 0.118 - 0.114(x - 0.047) \tag{18}$$

In the streamwise direction 201 grid points, in the normal direction 111 grid points, and during each period 100 steps were used for the unsteady calculation. The first grid point in the normal direction is placed within $y^+ = 1$. Four time periods have been calculated to eliminate the effects of initial condition. For both the high-frequency case and the low-frequency case, the time-averaged results from the two different turbulence models are found to be nearly identical, and both of them agree well with the measured data.

The predicted unsteady boundary-layer integral parameters are compared with the experimental data in Fig. 4. As suggested by Cousteix and Houdeville,[1] the combination of convection of turbulence in the outer region of the boundary layer and the forced oscillation leads to a weakly damped spatial pseudoperiodicity in the development of the boundary-layer integral parameters. This phenomenon has been correctly captured by the numerical solution. The differences in predictions from the present model and Chien's[6] model are not significant for the integral parameters. The differences are not significant because the pseudoperiodicity depends mainly on the solutions in the outer region of the boundary layer, where these two models are nearly identical. It should be mentioned that the k,ε profile given at the initial station is only a crude approximation, which affects the growth rate of turbulence in the boundary layer. This approximation is believed to be the reason for the underprediction of the amplitude of the spatial oscillation in the initial part of the boundary layer, shown in Fig. 4a.

The predicted and measured unsteady wall shear stresses are compared in Fig. 5. For both the high-frequency case and the low-frequency case, the predicted amplitudes of wall shear stress from the present model lie within the range of the experimental data. However, Chien's[6] model overpredicts the amplitude at high frequency. At high frequency, both models predict the correct trend for the phase angle of the wall shear stress. For the low-frequency case, the present model correctly predicts the phase angle of wall shear stress, but Chien's[6] model gives an overprediction. Because the unsteady wall shear stress depends mainly on the near-wall flow physics, it can be deduced that the present model is able to correctly predict unsteady near-wall turbulent flows.

Prediction of Frequency Dependency of Near-Wall Turbulent Flows

To investigate the behavior of the present turbulence model in unsteady near-wall turbulent flows, an unsteady turbulent boundary layer on a flat plate has been computed. The amplitude of freestream velocity oscillation is 10% of the mean value and the Reynolds number is 10^6. The nondimensional frequency parameter l_s^+ is varied from 8 to 64. The boundary-layer profile for the near-wall region is compared with the near-wall region data for a chan-

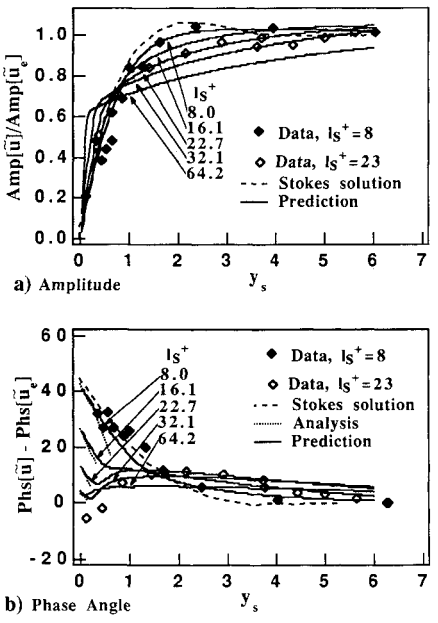

Fig. 6 Frequency dependency of unsteady velocity profile in a periodic boundary layer (data: Binder et al.[14]; analysis: Cousteix and Houdeville[1]).

nel flow tested by Binder et al.[14] Because the near-wall unsteady flow is controlled by the parameter l_s^+, the comparisons are made for identical l_s^+ values.

The variation in amplitude of the near-wall velocity profile with frequency is plotted in Fig. 6a. At high frequency, $l_s^+ = 8.0$, the solution approaches the laminar Stokes solution. This result is in agreement with the experimental observation by Binder et al.[14,21] The variation in amplitude is nearly confined to the viscous sublayer, whereas the outer layer is frozen ($\Delta u = \Delta u_e$). As frequency decreases, the profile of velocity amplitude departs from the laminar Stokes solution. At $l_s^+ = 22.7$, the calculated velocity amplitude agrees well with the data in the inner part of the boundary layer ($y_s \leq 3.7$). Beyond $y_s = 3.7$, the data show an unexpected abrupt downward shift, which is not predicted. The phase angle of the near-wall velocity profiles is shown in Fig. 6b. The predicted phase angle approaches the Stokes solutions at high frequency, with a 45-deg phase lead at the wall and a zero phase in the outer layer. This again confirms the observations by Binder et al.[14,21] As frequency decreases, the phase angle at the wall decreases whereas the phase angle in the outer region increases slightly. At intermediate frequencies, a dip in the phase angle profile is observed in the near-wall region. As the frequency is reduced further, the flow approaches quasisteady state, and the phase angle approaches zero in the entire boundary layer.

For $l_s^+ = 22.7$, the predicted phase angle agrees well with the data in the range $1 \leq y_s \leq 3.7$. Beyond $y_s = 3.7$, the predicted phase angle is 3–4 deg greater than the data. The data again show an abrupt downward shift at this location. For $y_s < 1$, the data show a monotonic increase in the phase angle with the normal distance, however, the numerical prediction suggests a trend that is first decreasing and then increasing.

In the viscous sublayer, an approximate analytic solution for the velocity phase shift has been given by Cousteix and Houdeville[1] as

$$\tan(\mathrm{Phs}[\tilde{u}] - \mathrm{Phs}[\tilde{u}_e]) = \tan(\mathrm{Phs}[\tau_w] - \mathrm{Phs}[\tilde{u}_e])$$

$$-\frac{\bar{\omega}\nu}{2\bar{u}_e^2}\left(\frac{\bar{C}_f}{2}\right)^{-3/2} \frac{\mathrm{Amp}[\tilde{u}_e]/\bar{u}_e}{\mathrm{Amp}[\tau_w]/\bar{\tau}_w} \frac{\bar{y}^+}{\cos(\mathrm{Phs}\tau_w - \mathrm{Phs}[\tilde{u}_e])} \tag{19}$$

This equation shows that the velocity phase shift is not constant near the wall, but decreases with increasing y. The results from this equation are plotted in Fig. 6b for $\bar{y}^+ \leq 5$, using the computed

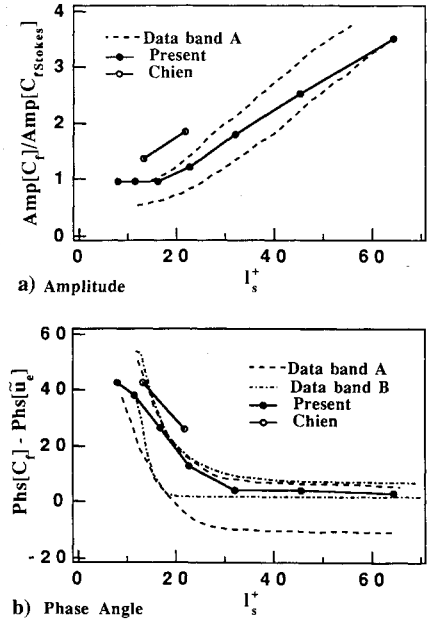

Fig. 7 Frequency dependency of unsteady skin friction in a periodic boundary layer (data band A: Binder et al.[14]; data band B: Cousteix and Houdeville[1]).

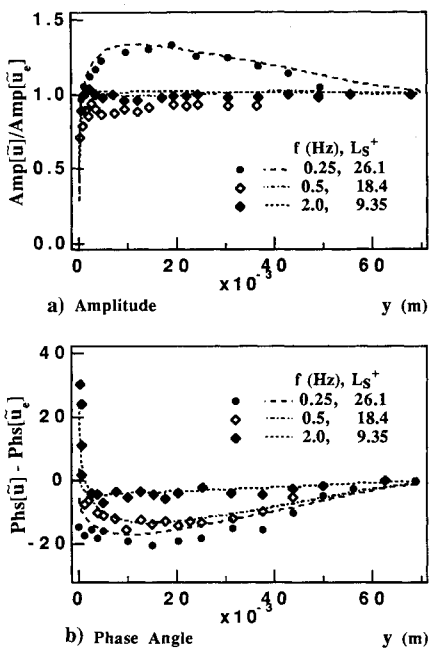

Fig. 8 Unsteady velocity profile in the outer region of a periodic turbulent boundary layer with adverse pressure gradient (symbols: data, Parikh et al.[15,16]; curves: prediction).

phase angles of the wall shear stress. The agreement between the predicted and the analytical variation in the velocity phase angle is good in the viscous sublayer, which indicates that the present model can correctly predict the near-wall unsteady flow.

It should be mentioned that the 38-Hz case measured by Cousteix and Houdeville[1] has an l_s^+ value of 22. A phase lead of nearly 12 deg in the wall shear stress was measured, which agrees well with the predicted value of 13 deg for the $l_s^+ = 22.7$ case. Furthermore, Cousteix and Houdeville[1] have reported that the logarithmic law exists for the instantaneous velocity profile at this frequency. The existence of the logarithmic law implies that the phase angle in velocity is nearly constant in the logarithmic region and is equal to the phase angle of the velocity at the wall. This implication is possible only if there is a dip on the near-wall velocity phase profile. This phenomenon is confirmed by the numerical prediction.

The variation in amplitude and phase angle of the wall shear stress with the nondimensional parameter l_s^+ is shown in Fig. 7. The predicted values for Cousteix and Houdeville's[1] cases using Chien's[6] model are also plotted for comparison. At the high-frequency limit, the predicted nondimensional amplitude approaches unity and the phase angle approaches 45 deg, indicating a near-wall flow approaching the laminar Stokes solution. The predicted results lie within the data bands given by Cousteix and Houdeville[26] and Binder et al.[14] This indicates that the present model is capable of predicting the unsteady wall shear stress at different frequencies to an engineering accuracy. Chien's[6] model overpredicts the amplitude at high frequency and the phase angle at intermediate frequency.

Unsteady Turbulent Boundary Layer with Adverse Pressure Gradients

The unsteady turbulent boundary-layer data by Parikh et al.[15,16] has been used to test the capability of the present turbulence model to predict the unsteady turbulent boundary layers with pressure gradients. The freestream velocity is given by

$$\tilde{u}_e/\bar{u}_e = 1 \qquad x < x_0$$

$$= 1 - 0.05\frac{x - x_0}{L}[1 - \cos(\omega t)] \qquad x_0 < x < x_0 + L \tag{20}$$

where L is the length of the test section. Velocity and frequency scaling have been carried out to simulate the test data acquired in a

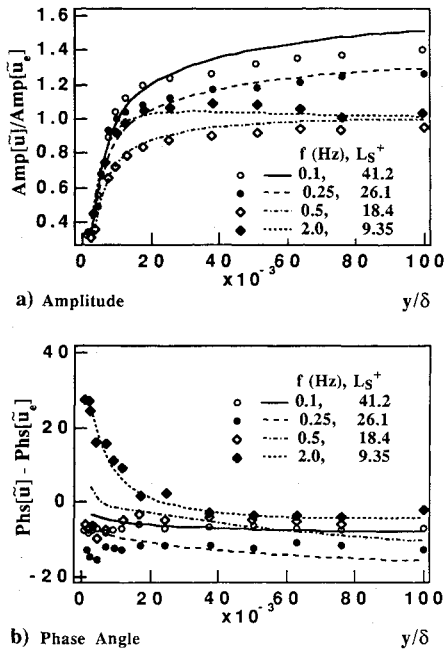

Fig. 9 Unsteady velocity profile in the near-wall region of a periodic turbulent boundary layer with adverse pressure gradient (symbols: data, Parikh et al. [15,16]; curves: prediction).

water tunnel. The Reynolds number and reduced frequency are kept nearly the same as the measured values.

Figure 8 shows the amplitude and the phase angle of the velocity in the outer region. At frequency $f = 0.25$ Hz, both the large overshoot in the velocity amplitude and the large negative phase angle are correctly predicted. The increase in frequency to $f = 0.5$ Hz causes a drastic reduction in the overshoot of the amplitude and a decrease in the absolute phase angle. The predicted phase angles agree well with the data, but the amplitude is slightly overpredicted. At high frequency, $f = 2$ Hz, both the prediction and the data indicate that the outer part of the boundary layer is frozen, with nearly zero phase angle and an amplitude of near unity. The overshoot in the amplitude becomes small and is confined to the near-wall region.

Figure 9 shows the profiles of amplitude and phase angle of velocity in the near-wall region. The variation in the amplitude and the phase angle in the near-wall region is well predicted. At $f = 0.1$ Hz, there is a large overshoot in the amplitude profile. The overshoot becomes smaller as the frequency increases to 0.25 Hz. At $f = 0.5$, the overshoot disappears completely in the near-wall region. As frequency reaches $f = 2$ Hz, small overshoot near the wall appears again, which is similar to the Stokes solution. The phase angle in the outer portion of the near-wall region is nearly constant at all frequencies shown, with a small negative value at low and high frequencies and a relatively larger negative value at $f = 0.25$ Hz. In the inner portion of the near-wall region, both the numerical prediction and the experimented data show a large phase lead at high frequency. At lower frequencies, numerical results indicate a decrease of phase shift with increasing y within the viscous sublayer. This result agrees with the analysis by Cousteix and Houdeville.[1] Because the velocity amplitudes are small, some uncertainties in the measured velocity phase angles might exist in the viscous sublayer.

Concluding Remarks

The analysis and computation carried out in this paper indicate that the local turbulent Reynolds numbers R_y and R_t, instead of the inner variable y^+, should be used to formulate the near-wall and low-Reynolds-number functions in a low-Reynolds-number k-ε model for unsteady turbulent flows. More stringent requirements should be placed on the near-wall asymptotic behavior of the near-wall and low-Reynolds-number functions.

A new low-Reynolds-number turbulence model has been developed for unsteady wall bounded flows. The near-wall and low-Reynolds-number functions are correlated with R_y and R_t, and the near-wall asymptotic behavior of turbulence quantities is ensured.

The present model accurately predicts steady turbulent boundary layers. For unsteady turbulent boundary layers, significant improvement has been achieved in simulating the near-wall flows. The new model correctly predicts the unsteady near-wall velocity profile and the unsteady skin friction in periodic turbulent boundary layers at different frequencies, with and without adverse pressure gradients.

Acknowledgments

This work was supported by NASA through the Contract NAG 3-1168, with P. Sockol as the technical monitor. The unsteady boundary-layer code (UNSVIS) used in this investigation was developed by G. D. Power, J. M. Verdon, K. A. Kousen, and M. Barnett.

References

[1]Cousteix, J., and Houdeville, R., "Effects of Unsteadiness on Turbulent Boundary Layers," von Karman Inst. for Fluid Dynamics, Lecture Series 1983–03, Feb.–March 1983.

[2]Power, G. D., Verdon, J. M., and Kousen, K. A., "Analysis of Unsteady Compressible Viscous Layers," *Transactions of the American Society of Mechanical Engineers, Journal of Turbomachinery,* Vol. 133, No. 4, 1991, pp. 644–653.

[3]Mankbadi, R. R., and Mobark, A., "Quasi-steady Turbulence Modeling of Unsteady Flows," *International Journal of Heat and Fluid Flow,* Vol. 12, No. 2, 1991, pp. 122–129.

[4]Justesen, P., and Spalart, P. R., "Two-Equation Turbulence Modeling of Oscillatory Boundary Layers," AIAA Paper 90-0496, Jan. 1990.

[5]Jones, W. P., and Launder, B. E., "The Prediction of Laminarization with a Two-Equation Model of Turbulence," *International Journal of Heat and Mass Transfer,* Vol. 15, Feb. 1972, pp. 301–314.

[6]Chien, K. Y., "Predictions of Channel and Boundary-Layer Flows with a Low-Reynolds-Number Turbulence Model," *AIAA Journal,* Vol. 20, No. 1, 1982, pp. 33–38.

[7]Hanjalic, K., and Stosic, N., "Hysteresis of Turbulent Stresses in Wall Flows Subjected to Periodic Disturbances," *Fourth Symposium on Turbulent Shear Flows,* Karlsruhe, Germany, Sept. 1983, pp. 287–300.

[8]Kebede, W., Launder, B. E., and Younis, B. A., "Large-amplitude Periodic Pipe Flow: A Second-moment Closure Study," *Fifth Symposium on Turbulent Shear Flows,* Toulouse, France, Sept. 1987, pp. 16.23–16.29.

[9]Ha Minh, H., Viegas, J. R., Rubesin, M. W., Vandromme, D. D., and Spalart, P., "Physical Analysis and Second-Order Modeling of an Unsteady Turbulent Flow: The Oscillating Boundary Layer on a Flat Plate," *Seventh Symposium on Turbulent Shear Flows,* Stanford, CA, Aug. 1989, pp. 11.5.1–11.5.6.

[10]Cousteix, J., Desopper, A., and Houdeville, R., "Structure and Development of a Turbulent Boundary Layer in an Oscillatory External Flow," *First Symposium on Turbulent Shear Flows,* PA, April 1977, pp. 154–171.

[11]Wieghardt, K., and Tillmann, W., "On the Turbulent Friction Layer for Rising Pressure," NACA TM-1314, 1951.

[12]Cousteix, J., Houdeville, R., and Javelle, J., "Response of a Turbulent Boundary Layer to a Pulsation of the External Flow with and without Adverse Pressure Gradient," *International Union of Theoretical and Applied Mechanics, Symposium on Unsteady Turbulent Shear Flows,* Springer-Verlag, Berlin, 1981, pp. 120–144.

[13]Cousteix, J., Javelle, J., and Houdeville, R., "Influence of Strouhal Number in the Structure of Flat Plate Turbulent Boundary Layer," *Third International Symposium on Turbulent Shear Flows,* Univ. of California, Davis, CA, Sept. 9–11, 1981, pp. 46–53.

[14]Binder, G., Tardu, S., Blackwelder, R. F., and Kueny, J. L., "Large Amplitude Periodic Oscillations in the Wall Region of a Turbulent Channel Flow," *Fifth Symposium on Turbulent Shear Flow,* Cornell Univ., Ithaca, NY, Aug. 1985, pp. 16.1–16.7.

[15]Parikh, P. G., Jayaraman, R., and Reynolds, W. C., "Dynamics of an Unsteady Turbulent Boundary-Layer," *Proceedings of the Third Symposium on Turbulent Shear Flows,* Univ. of California, Davis, CA, 1981, pp. 8.35–8.40.

[16]Parikh, P. G., Reynolds, W. C., Jayaraman, R., and Carr, L.W., "Dynamic Behavior of an Unsteady Turbulent Boundary Layer," *International Union of Theoretical and Applied Mechanics, Symposium on Unsteady Turbulent Shear Flows,* Springer-Verlag, Berlin, 1981, pp. 35–46.

[17]Patel, C. V., Rodi, W., and Scheuerer, G., "Turbulence Models for Near-Wall and Low Reynolds Number Flows: A Review," *AIAA Journal,* Vol. 23, No. 9, 1985, pp. 1308–1319.

[18]Lam, C. K. G., and Bremhorst, K., "A Modified Form of the k-ε Model for Predicting Wall Turbulence," *Transactions of the American Society of Mechanical Engineeris, Journal of Fluids Engineers*, Vol. 103, Sept. 1981, pp. 456–459.

[19]Myong, H. K., and Kasagi, N., "A New Approach to the Improvement of k-ε Turbulence Model for Wall Bounded Shear Flows," *Japanese Society of Mechanical Engineering International Journal*, Series II, Vol. 33, No. 1, 1990, pp. 63–72.

[20]Nagano, Y., and Hishida, M., "Improved Form of the k-ε Model for Turbulent Shear Flows," *Transactions of the American Society of Mechanical Engineers*, Vol. 109, June 1987, pp. 156–160.

[21]Binder, G., and Kueny, J. L., "Measurements of the Periodic Velocity Oscillations Near the Wall in Unsteady Turbulent Channel Flow," *Proceedings of the Third Symposium on Turbulent Shear Flows*, Univ. of California, Davis, CA, 1981, pp. 8.19–8.25.

[22]Lai, Y. G., and So, R. M. C., "On Near-wall Turbulent Flow Modeling," *Journal of Fluid Mechanics*, Vol. 221, Dec. 1990, pp. 641–673.

[23]Speziale, C. G., Abid, R., and Anderson, E. C., "A Critical Evaluation of Two-Equation Models for Near Wall Turbulence," *AIAA Journal*, Vol. 30, No. 2, 1992, pp. 324–331.

[24]Hanjalic, K., and Launder, B. E., "Contribution Towards a Reynolds-Stress Closure for Low-Reynolds-Number Turbulence," *Journal of Fluid Mechanics*, Vol. 74, March 1976, p. 593.

[25]Schmidt, R. C., and Patankar, S. V., "Simulating Boundary Layer Transition with Low-Reynolds-Number k-ε Turbulence Models: Part 1—An Evaluation of Prediction Characteristics, Part 2—An Approach to Improving the Predictions," *Transactions of the American Society of Mechanical Engineers, Journal of Fluids Engineering*, Vol. 113, Jan. 1991, pp. 10–26.

[26]Cousteix J., and Houdeville, R., "Turbulence and Skin Friction Evolutions in an Oscillating Boundary Layer," *Fifth Symposium on Turbulent Shear Flow*, Cornell Univ., Ithaca, NY, Aug. 1985, pp. 18.7–18.12.